



THE UNIVERSITY *of* EDINBURGH

## Edinburgh Research Explorer

### Human pericytes for ischemic heart repair

**Citation for published version:**

Chen, C-W, Okada, M, Proto, JD, Gao, X, Sekiya, N, Beckman, SA, Corselli, M, Crisan, M, Saparov, A, Tobita, K, Péault, B & Huard, J 2013, 'Human pericytes for ischemic heart repair', *STEM CELLS*, vol. 31, no. 2, pp. 305-316. <https://doi.org/10.1002/stem.1285>

**Digital Object Identifier (DOI):**

[10.1002/stem.1285](https://doi.org/10.1002/stem.1285)

**Link:**

[Link to publication record in Edinburgh Research Explorer](#)

**Document Version:**

Peer reviewed version

**Published In:**

STEM CELLS

**Publisher Rights Statement:**

Published in final edited form as:  
Stem Cells. Feb 2013; 31(2): 305–316.  
doi: 10.1002/stem.1285

**General rights**

Copyright for the publications made accessible via the Edinburgh Research Explorer is retained by the author(s) and / or other copyright owners and it is a condition of accessing these publications that users recognise and abide by the legal requirements associated with these rights.

**Take down policy**

The University of Edinburgh has made every reasonable effort to ensure that Edinburgh Research Explorer content complies with UK legislation. If you believe that the public display of this file breaches copyright please contact [openaccess@ed.ac.uk](mailto:openaccess@ed.ac.uk) providing details, and we will remove access to the work immediately and investigate your claim.



Published in final edited form as:

*Stem Cells*. 2013 February ; 31(2): 305–316. doi:10.1002/stem.1285.

## Human Pericytes for Ischemic Heart Repair

Chien-Wen Chen, MD, PhD<sup>1,2,7</sup>, Masaho Okada, MD, PhD<sup>2,7</sup>, Jonathan D. Proto, BS<sup>2,6,7,\*</sup>, Xueqin Gao, MD, PhD<sup>2,7,\*</sup>, Naosumi Sekiya, MD, PhD<sup>2,5,7,\*</sup>, Sarah A. Beckman, BS<sup>2,6,7</sup>, Mirko Corselli, PhD<sup>9</sup>, Mihaela Crisan, PhD<sup>10</sup>, Arman Saparov, MD, PhD<sup>11</sup>, Kimimasa Tobita, MD<sup>3,4,8</sup>, Bruno Péault, PhD<sup>9,12</sup>, and Johnny Huard, PhD<sup>2,7,8</sup>

<sup>1</sup>Department of Bioengineering, University of Pittsburgh <sup>2</sup>Department of Orthopaedic Surgery, University of Pittsburgh <sup>3</sup>Department of Pediatrics, University of Pittsburgh <sup>4</sup>Department of Developmental Biology, University of Pittsburgh <sup>5</sup>Department of Surgery, University of Pittsburgh <sup>6</sup>Department of Pathology, University of Pittsburgh <sup>7</sup>Stem Cell Research Center, University of Pittsburgh <sup>8</sup>McGowan Institute for Regenerative Medicine, University of Pittsburgh <sup>9</sup>UCLA Orthopaedic Hospital, Department of Orthopaedic Surgery, and the Orthopaedic Hospital Research Center, University of California at Los Angeles, USA <sup>10</sup>Erasmus MC Stem Cell Institute, Department of Cell Biology, Rotterdam, The Netherlands <sup>11</sup>Center for Energy Research, Nazarbayev University, Kazakhstan <sup>12</sup>Centre for Cardiovascular Science and Centre for Regenerative Medicine, University of Edinburgh, UK

### Abstract

Human microvascular pericytes (CD146<sup>+</sup>/34<sup>+</sup>/45<sup>+</sup>/56<sup>+</sup>) contain multipotent precursors and repair/regenerate defective tissues, notably skeletal muscle. However, their ability to repair the ischemic heart remains unknown. We investigated the therapeutic potential of human pericytes, purified from skeletal muscle, for treating ischemic heart disease and mediating associated repair mechanisms in mice. Echocardiography revealed that pericyte transplantation attenuated left ventricular dilatation and significantly improved cardiac contractility, superior to CD56<sup>+</sup> myogenic progenitor transplantation, in acutely infarcted mouse hearts. Pericyte treatment substantially reduced myocardial fibrosis and significantly diminished infiltration of host inflammatory cells at the infarct site. Hypoxic pericyte-conditioned medium suppressed murine fibroblast proliferation and inhibited macrophage proliferation *in vitro*. High expression by pericytes of immunoregulatory molecules, including IL-6, LIF, COX-2 and HMOX-1, was sustained under hypoxia, except for MCP-1. Host angiogenesis was significantly increased. Pericytes supported microvascular structures *in vivo* and formed capillary-like networks with/without endothelial cells in three-dimensional co-cultures. Under hypoxia, pericytes dramatically increased expression of VEGF-A, PDGF- $\beta$ , TGF- $\beta$ 1 and corresponding receptors while expression of bFGF, HGF, EGF, and Ang-1 was repressed. The capacity of pericytes to

Correspondence to: Johnny Huard, Ph.D., Stem Cell Research Center, Department of Orthopaedic Surgery, University of Pittsburgh School of Medicine, 206 Bridgeside Point II, 450 Technology Drive, Pittsburgh, PA15219, USA, Tel: (412) 648-2798, Fax: (412) 648-4066, jhuard@pitt.edu.

\*These authors contributed equally;

### Disclosure of Conflicts of Interest

J.H. received remuneration from Cook MyoSite, Inc. for consulting services and for royalties received from technology licensing during the period that the above research was performed. All other authors have no conflict of interest to disclose.

Author contributions: C.W.C.: designed and performed research, analyzed data, and wrote the manuscript. M.O.: performed research and analyzed data. J.D.P.: performed research and analyzed data. X.G.: performed research and analyzed data. N.S.: performed research. S.A.B.: performed research and analyzed data. M. Corselli performed research. M. Crisan performed research. A.S. participated in experimental design and provided funding. K.T.: designed and performed research. B.P.: designed research, provided funding, and edited the manuscript. J.H.: designed research, provided funding, edited and approved the manuscript.

See [www.StemCells.com](http://www.StemCells.com) for supporting information available online.

differentiate into and/or fuse with cardiac cells was revealed by GFP-labeling, though to a minor extent. In conclusion, intramyocardial transplantation of purified human pericytes promotes functional and structural recovery, attributable to multiple mechanisms involving paracrine effects and cellular interactions.

## Keywords

pericytes; angiogenesis; immunomodulation; myocardial infarction; stem cell therapy

## Introduction

Coronary heart disease (CHD) is the leading cause of death in the United States, affecting 16.3 million people and accounting for 1 of every 3 deaths in 2007 [1]. Prolonged pathological interference with the coronary blood supply, such as atherosclerosis and thromboemboli, results in ischemic cardiomyopathy and/or myocardial infarction (MI) [2]. MI often leads to heart failure (HF) due to the limited capacity of the human heart to repair/regenerate its damaged myocardium [2,3]. As an alternative to heart transplantation, stem/progenitor cell therapy (SCT) is deemed promising for restoration of cardiac function and prevention of progressive HF [3,4]. In particular, human bone marrow precursor cells, endothelial progenitor cells, skeletal myoblasts, and endogenous cardiac progenitor cells, have been intensively investigated with uneven success in pre-clinical and clinical trials [3–6]. Given the vascular origin of CHD pathology, stem/progenitor cells capable of reconstituting host vascular networks, in addition to other merits, will be ideal cell sources for SCT.

Microvascular pericytes (aka mural cells or Rouget cells) that tightly encircle capillaries and microvessels (arterioles and venules) and regulate microvascular physiology have recently been shown to contain precursor cells endowed with mesodermal differentiation potential [7]. Pericytes (CD146<sup>+</sup>/34<sup>-</sup>/45<sup>-</sup>/56<sup>-</sup>) purified by cell sorting from human skeletal muscle, adipose, placenta, pancreas and other organs repair and regenerate damaged/defective tissues [8–12] and represent the CD146-positive developmental origin of the heterogeneous mesenchymal stem/stromal cells (MSCs) [12–16]. Owing to their wide distribution in the microvasculature, pericytes are regarded as a promising and attractive source of precursor cells for regenerative medicine [17–19]. We hypothesize SCT with purified pericytes to be a suitable approach for the treatment of ischemic heart disease (IHD) [20].

Besides cardiomyogenesis, cardioprotective mechanisms, including anti-fibrosis, anti-inflammation, and neovascularization, play critical roles in SCT-mediated cardiac repair following ischemic insults [21–23]. SCT reduces myocardial fibrosis and induces favorable tissue remodeling in the ischemic heart, which in turn increases myocardial compliance/strength and prevents the progressive, pathological decline toward HF [24,25]. This anti-fibrotic feature was attributed in part to increased collagen degradation by matrix metalloproteinases (MMPs) and inhibition of fibroblast activation, possibly through a paracrine mechanism [26,27]. Additionally, the immunosuppressive/anti-inflammatory capacity of MSCs through secretion of immunoregulatory molecules has recently attracted clinical attention in organ transplantation and immune regulation [28,29]. Whether pericytes possess similar anti-fibrotic and immunoregulatory capacities within the ischemic microenvironment remains to be addressed.

To relieve the underlying cause of IHD, SCT-based approaches toward myocardial revascularization have been extensively pursued [30,31]. Due to their native vascular localization and secretion of trophic factors that are associated with tissue repair and

vascular growth/remodeling, pericytes may restore injured vascular networks more efficiently [18]. Pro-angiogenic signaling molecules released by stem/progenitor cells stimulate neovascularization in ischemic tissues [31]. Additionally, cell-cell interaction between vascular mural cells and endothelial cells was lately suggested to play essential roles in blood vessel remodeling and maturation [32,33]. Whether pericytes mediate revascularization of the ischemic myocardium through any of these two mechanisms has yet to be tested

In the present study, we investigated the therapeutic potential of purified human skeletal muscle pericytes in IHD, using an acute MI (AMI) model in immunodeficient mice. Transplantation of pericytes not only reversed cardiac dilatation but also improved cardiac contractility. Major repair mechanisms were investigated, including reduction of fibrosis, inhibition of chronic inflammation, promotion of angiogenesis, and regeneration of the myocardium. We further describe putative mediators employed by pericytes. GFP-labeling was used to track perivascular homing and lineage fate of transplanted pericytes. Our results demonstrate that the overall benefit of pericyte treatment is collectively attributed to multiple cardioprotective mechanisms that involve paracrine and direct cell-cell interactions.

## Material and Methods

### Human Tissue Biopsies and Cell Isolation

In total, 3 independent human skeletal muscle specimens (1 adult and 2 fetal) were used for cell isolation. The procurement of adult muscle biopsies from the National Disease Research Interchange was approved by the Institutional Review Board (IRB) at the University of Pittsburgh. Muscle biopsies (male subject, 57 years old) were preserved in DMEM containing 1% antibiotics and transported to the laboratory on ice. Human fetal tissues (21 and 23 weeks of gestation) were obtained following voluntary pregnancy interruptions performed at Magee Womens Hospital, Pittsburgh, in compliance with IRB protocol 0506176. Informed consents for the use of fetal tissues were obtained from all patients. Cells were mechanically and enzymatically dissociated from muscle biopsies following the reported protocol [12]. Details are described in supplemental material.

### Fluorescence-activated Cell Sorting (FACS) and Flow Cytometry Analysis

FACS and flow cytometry were used to purify microvascular pericytes ( $CD146^{+}/34^{-}/45^{-}/56^{-}$ ) and examine cell lineage marker expression respectively, as we previously reported [12]. Details are documented in supplemental material.

### Cell Culture and Cell Labeling

Sorted pericytes were expanded in reported culture conditions [12]. Single donor-derived human umbilical cord vein endothelial cells (HUVECs, Lonza) were cultured in endothelial cell growth medium-2 (EGM-2, Lonza). Cultured pericytes were labelled with green fluorescence protein (GFP) following a published protocol [12], using a lentivirus-based CMV-driven eGFP-expression vector. For short-term experiments, cells were labelled with cell membrane dyes, PKH26 (red) and PKH67 (green) (both from Sigma-Aldrich), and used immediately without further expansion.

### Cell Transplantation in an Acute Myocardial Infarction Model

The Institutional Animal Care and Use Committee at Children's Hospital of Pittsburgh and University of Pittsburgh approved the animal usage and surgical procedures (Protocol#37-04, 55-07, 0901681A-5). A total of 78 male NOD/SCID mice (Jackson Laboratory) were used. MI induction (by ligation of left anterior descending coronary artery) and intramyocardial cell injection ( $3 \times 10^5$  cells/heart) were performed by a blinded surgeon

as previously reported [34]. Control mice received injections of 30  $\mu$ l phosphate-buffered saline (PBS).

### Evaluation of Cardiac Function by Echocardiography

Mice were anesthetized with isoflurane and transthoracic echocardiography was performed by a blinded investigator repeatedly before and after surgery (at 2 and 8 weeks), using a high resolution ultrasound system (Vevo 770, Visual Sonics), as described previously [34]. Mice which died prior to 8 weeks post-injection were excluded. Echocardiographic measurements are listed in supplemental material.

### Histological and Immunohistochemical Analyses

At 1, 2, and 8 weeks post-surgery, hearts were harvested and processed as previously described [34]. Cryosections at 6–8  $\mu$ m thickness were used for histological and immunohistochemical analyses following published protocols [34]. Anti-GFP immunofluorescent staining was performed on 4% paraformaldehyde-fixed sections. Donor cell engraftment and perivascular homing were quantified on serial sections stained with anti-GFP antibody (Abcam) and dual-stained with anti-GFP/anti-mouse CD31 (BD Biosciences) antibodies respectively, using Image J. The engraftment ratio was defined as the extrapolated total number of engrafted GFP-positive cells to the initial  $3 \times 10^5$  cells injected. Perivascular homing ratio was defined as the extrapolated number of GFP-positive cells juxtaposing CD31-positive mouse endothelial cells to the extrapolated total number of engrafted cells. Using Masson's trichrome staining (San Marcos), fibrotic area fraction and infarct wall thickness were estimated from 6 randomly selected sections at comparable infarct levels per heart as previously described [34]. Quantification of host angiogenesis and chronic inflammation was computed from 6–10 randomly selected images taken from the designated area in sections stained with anti-mouse CD31 and anti-mouse CD68 (Abcam) at the mid-infarct level respectively. Experimental details are documented in supplemental material.

### Hypoxia Assay and ELISA

To simulate the lower oxygen tension at the tissue level, physiologically or pathologically, pericytes were cultured under 2.5% O<sub>2</sub> hypoxic conditions (with 5% CO<sub>2</sub> and 92.5% N<sub>2</sub>) as formerly described [34]. Cells were washed twice before defined, serum-free DMEM medium was added upon the transition to low O<sub>2</sub> conditions. Culture supernatant and cell lysates were collected 24 hours later. Cells cultured under 21% O<sub>2</sub> (normoxia) served as controls. The secretion of vascular endothelial growth factor (VEGF), angiopoietin-1 (Ang-1), angiopoietin-2 (Ang-2), and transforming growth factor (TGF)- $\beta$ 1 in the culture supernatant was measured by respective enzyme-linked immunosorbent assay (ELISA) with human VEGF (Invitrogen), Ang-1, Ang-2, and TGF- $\beta$ 1 (all from R&D Systems) ELISA Kits.

### Real-time Quantitative PCR and Semi-quantitative RT-PCR

Real-time quantitative PCR (rt-qPCR) was performed as previously reported [9]. Total RNA (N=6) was extracted for cDNA synthesis. The quantitative analyses were performed in the core facility at the University of Pittsburgh. All data are presented as expression level normalized to human cyclophilin (in arbitrary fluorescence units). For semi-quantitative RT-PCR (sqRT-PCR), total RNA (N=3) were extracted using RNeasy plus-mini-kits (Qiagen). From each sample, 500ng of total RNA were reverse transcribed, followed by PCR. The intensity of the product bands were calculated using Quantify-One software and normalized to  $\beta$ -actin. The primer sequences are listed in supplemental table T1 and T2.

## In vitro Vascular Network Formation

Cell culture/co-culture experiments using 2D and 3D Matrigel systems were performed to observe the capillary-like network formation. For 2D culture,  $5 \times 10^4$  pericytes or HUVECs were seeded onto Matrigel-coated well and incubated for 24 hours. For 3D culture,  $25 \times 10^4$  pericytes or HUVECs were re-suspended in EGM-2 medium and mixed with Matrigel in a 3:1 ratio. The Matrigel plug was subsequently incubated for 72 hours. Equal numbers of dye-labeled pericytes and HUVECs were well mixed in 2D or 3D co-culture for 72 hours to observe pericyte-HUVEC interactions.

## Measurement of Cell Proliferation

Murine RAW264.7 monocyte/macrophage cells (ATCC) or primary murine skeletal myoblasts, muscle fibroblasts, and cardiac fibroblasts were cultured with normoxic or hypoxic pericyte-culture conditioned medium, or with serum-free control medium, for 72 hours. Cell proliferation was measured by the absorbance at 490nm after incubation with CellTiter Proliferation Assay Reagent (Promega) for 3 hours. Experiments were performed in quadruplicates and repeated 3 times independently.

## Statistical Analysis

All measured data are presented as mean  $\pm$  standard error (SE). Kaplan-Meier survival curve estimation with log-rank test was performed to compare the animal survival rate between treatment groups. Statistical differences were analyzed by Student's *t*-test (two groups), one-way ANOVA (multiple groups), or two-way repeated ANOVA (repeated echocardiographic measurements) with 95% confidence interval. Statistical significance was set at  $p < 0.05$ . Student-Newman-Keuls multiple comparison test (or Bonferroni test if specified) was performed for ANOVA post-hoc analysis. Statistical analyses were performed with SigmaStat 3.5 (Systat Software) and SPSS19 (IBM) statistics software.

## Results

### Isolation and Transplantation of Human Pericytes

As reported in our previous studies [12], FACS was used to purify human microvascular pericytes ( $CD146^{+}/34^{-}/45^{-}/56^{-}$ ) to homogeneity from skeletal muscle biopsies of three donors (one adult and two fetal, designated as AP, FP1, and FP2 respectively), by their differential expression of cell lineage markers, including CD34 (endothelial/stem cells), CD45 (hematolymphoid cells), CD56 (myogenic cells), and CD146 (pericyte/endothelial cells) (Supplemental Figure S1). No phenotypical difference between adult and fetal pericytes was noted, consistent with our previous observations [12]. After *in vitro* expansion (25–35 cell doublings) and prior to transplantation, in all three pericyte populations, we have observed no alteration to their distinctive morphology as well as classic antigenic profile, including robust expression of CD146, alkaline phosphatase (ALP), and typical MSC markers: CD44, CD73, CD90, CD105 with the absence of CD34, CD45, and CD56 (Supplemental Figure S2A and S2B). Additionally, cell labeling (in subsequent experiments) did not alter pericyte phenotype (data not shown). Cells ( $3.0 \times 10^5$  cells/heart) resuspended in 30  $\mu$ l PBS were injected into the acutely infarcted myocardium of immunodeficient mice. The control group received injections of 30  $\mu$ l PBS following the induction of MI.

### Human Pericyte Transplantation Improves Cardiac Function

The survival of animals receiving pericyte treatment or PBS injection was monitored over the course of 8 weeks (Kaplan-Meier survival curve, log-rank test  $p = 0.529$ , Figure 1A). Cardiac function was assessed by echocardiography performed repeatedly before (healthy)



and at 2 and 8 weeks after surgery (Supplemental Figure S3). Ischemic hearts injected with either of the three pericyte populations (N=8 per donor) had significantly smaller left ventricular (LV) chamber size, as measured by LV end-diastolic area (LVEDA, Figure 1B) and end-systolic area (LVESA, Figure 1C), than the control group (N=8) (all  $p<0.05$ ), suggesting the reversal of progressive heart dilatation. Moreover, all pericyte-transplantation groups displayed significantly better LV contraction, evaluated by LV fraction shortening (LVFS, Figure 1D), LV fractional area change (LVFAC, Figure 1E), and LV ejection fraction (LVEF, Figure 1F), than the control group (all  $p<0.05$ ). Collectively, when compared to vehicle treatment, pericyte treatment not only resulted in considerably smaller LV chamber dimension ( $p<0.001$ , two-way repeated ANOVA) but also notably improved LV contractility ( $p<0.001$ , two-way repeated ANOVA) for up to 2 months. Dimensional and functional echocardiographic parameters are documented in Supplemental Table T3. In a separate experiment, we compared cardiac function of acutely infarcted hearts injected with either APs or CD56+ myogenic progenitors, sorted from a single adult muscle biopsy. The echocardiographic results at 2 weeks post-infarction showed that pericyte-treated hearts (N=6) have significantly better LV function than CD56+ progenitor-treated ones (N=6) in five parameters examined, including LVEDA ( $p=0.004$ ), LVESA ( $p=0.002$ ), LVFS ( $p=0.003$ ), LVFAC ( $p=0.003$ ), and LVEF ( $p=0.001$ ) (Supplemental Figure S4).

### Transplantation of Pericytes Reduces Cardiac Fibrosis

To understand the influence of pericyte treatment on cardiac fibrosis, we evaluated scar tissue formation using Masson's trichrome histological staining. At 2 weeks post-infarction, pericyte-treated hearts displayed less collagen deposition (stained in blue/purple) at the ischemic area (Figure 2A). Estimation of the total fibrotic tissue ratio unveiled a 45.3% reduction of cardiac fibrosis in the pericyte-injected myocardium (N=5,  $22.03\pm1.81\%$ ) when comparing to saline-injected controls (N=5,  $40.28\pm2.15\%$ ) (Figure 2B,  $p=0.001$ ), suggesting the anti-fibrotic efficacy of pericytes. Measurement of LV wall thickness at the center of the infarct indicated no significant difference ( $p>0.05$ ) between the pericyte group ( $0.255\pm0.026$  mm) and the PBS group ( $0.202\pm0.040$  mm), suggesting that pericytes had limited beneficial effects to reduce transmural infarct thinning following MI (Figure 2C).

### Paracrine Anti-fibrotic Effects of Pericytes under Hypoxia

Oxygen tension within tissues, physiologically or pathologically, is considerably lower than the ambient oxygen concentration *in vitro*. To elucidate the mechanism involved in pericyte-mediated reduction of fibrosis, we mimicked, at least in part, the hostile hypoxic microenvironment that donor cells encounter within the ischemic myocardium by culturing pericytes under 2.5% oxygen for 24 hours in defined, serum-free medium. Pericytes cultured under 21% oxygen (normoxia) served as controls. We then performed a cell proliferation assay using primary murine skeletal muscle and cardiac fibroblasts as well as skeletal myoblasts cultured with pericyte-conditioned medium (P-CM). Cardiac fibroblast proliferation was significantly reduced when cultured in hypoxic P-CM, compared to normoxic P-CM ( $p=0.019$ ) (Figure 2D). Muscle fibroblast proliferation exhibited the same inhibitory pattern ( $p<0.001$ , hypoxic versus normoxic P-CM) with normoxic P-CM showing a pro-proliferative effect over control serum-free medium ( $p<0.05$ ) (Figure 2D). Neither of the two P-CMs had significant influence over skeletal myoblast proliferation ( $p=0.76$ ). One-way ANOVA with Bonferroni multiple comparisons was performed for statistical analysis. This suggests a paracrine anti-fibrotic effect by pericytes in hypoxia. We further proposed a fibrolytic role of pericyte-derived matrix metalloproteinases (MMPs) and examined gene expression of MMP-2 and MMP-9 by real-time qPCR. Cultured pericytes expressed more MMP-2 but nearly 10 times less MMP-9 than total skeletal muscle lysates (tissue origin control) (Figure 2E). We then explored MMP expression in hypoxia-cultured pericytes and demonstrated that MMP-2 expression in pericytes was well sustained under 2.5% oxygen,

compared to normoxic culture (Figure 2F,  $p>0.05$ ), while MMP-9 expression remained extremely low without significant change (Figure 2F,  $p>0.05$ ). Immunohistochemical study revealed that some of the transplanted pericytes within the infarct region expressed MMP-2 (Figure 2G, a–d).

### Transplantation of Pericytes Inhibits Chronic Inflammation

Histological analysis of pericyte- and PBS-injected hearts after hematoxylin and eosin (H&E) staining indicated an increased focal infiltration of inflammatory cells (cluster of cells with dark blue-stained nuclei) within the infarct region in the latter (Figure 3A). To more precisely evaluate the immunomodulatory effect of pericyte transplantation, we detected host CD68-positive monocytes/macrophages by immunohistochemistry. Pericyte-injected hearts exhibited diminished infiltration of host phagocytic cells within the infarct region at 2 weeks post-infarction (Figure 3B). Districts of the myocardium unaffected by the ischemic insult (posterior and septal walls) contained few CD68-positive cells in either group, similar to healthy hearts (Figure 3C). Quantitatively, injection of pericytes ( $N=5$ ) resulted in a 34% reduction in infiltration of CD68-positive cells at 2 weeks post-infarction when compared to PBS controls ( $N=5$ ) (Figure 3D,  $p<0.001$ ).

### Paracrine Immunomodulation by Pericytes

To understand the underlying mechanism of pericyte-induced inhibition of phagocytic cell infiltration, we analyzed the proliferation of murine macrophages cultured with pericyte-conditioned medium. Murine macrophage proliferation was significantly inhibited when culturing with both normoxic ( $p=0.018$ ) and hypoxic ( $p<0.001$ ) pericyte-conditioned media, compared to control medium (Figure 3E). Furthermore, hypoxic pericyte-conditioned medium exhibited a more prominent immunomodulatory effect than the normoxic counterpart (Figure 3E,  $p=0.002$ ). We then investigated by sqRT-PCR the differential expression of genes encoding immunoregulatory molecules that are potentially accountable for this paracrine immunomodulation by pericytes. Under either normoxia or hypoxia, pericytes indeed expressed a considerable array of anti-inflammatory cytokines: interleukin-6 (IL-6), leukemia inhibitory factor (LIF), cyclooxygenase-2 (COX-2/PTGS-2, prostaglandin endoperoxide synthase-2) and heme oxygenase-1 (HMOX-1) (Figure 3F). Similarly, monocyte chemotactic protein-1 (MCP-1) and hypoxia-inducible factor-1 $\alpha$  (HIF-1 $\alpha$ ) were highly expressed by pericytes (Figure 3F). Conversely, we detected very low to no expression of pro-inflammatory cytokines including interleukin-1 $\alpha$  (IL-1 $\alpha$ ), tumor necrosis factor- $\alpha$  (TNF- $\alpha$ ), and interferon- $\gamma$  (IFN $\gamma$ ) (Figure 3F). No expression of interleukin-4 (IL-4), interleukin-10 (IL-10), inducible nitric oxide synthase (iNOS), and indoleamine 2,3-dioxygenase (2,3-IDO) was observed (Figure 3F). Quantitatively, there was no significant alteration of expression under hypoxia of immunoregulatory genes investigated, except MCP-1, whose expression was notably decreased in hypoxia-cultured pericytes (Figure 3G, all  $p>0.05$ ; MCP-1,  $p=0.027$ ).

### Transplanted Pericytes Promote Host Angiogenesis

We examined whether intramyocardial transplantation of pericytes restores the host vascular network post-infarction. Capillaries in the peri-infarct areas (Figure 4A) and within the infarct region (Figure 4B) were revealed by anti-mouse CD31 (platelet endothelial cell adhesion molecule, PECAM-1) immunofluorescent staining and subsequently quantified. Capillary structure density in the peri-infarct areas of pericyte-injected hearts ( $N=5$ ) was increased by 45.4% when compared to PBS-injected controls ( $N=5$ ) (Figure 4C,  $p=0.01$ ). Higher microvascular density was also observed within the infarct region, with 34.8% more capillaries in the pericyte-treated hearts (Figure 4C,  $p=0.002$ ). Detection of the proliferating host ECs by Ki-67, a cell proliferation marker, and CD31 showed that pericyte-injected hearts ( $N=3$ ) had significantly more proliferating ECs than PBS-injected controls ( $N=3$ ) in



both the infarct region ( $p=0.034$ ) and peri-infarct areas ( $p=0.025$ ) (Supplemental Figure S5A–C). These findings suggest that transplanted pericytes promote host angiogenesis not only in the peri-infarct areas, where blood vessels were generally better preserved after the ischemic injury, but also within the blood vessel-deprived infarct region.

### Pericytes Support Microvascular Structures

To demonstrate that pericytes benefit host vascular networks through their support of microvascular structures, we developed 2D and 3D Matrigel cultures/co-cultures using pericytes and HUVECs. HUVECs seeded onto Matrigel-coated wells formed typical capillary-like networks after 24 hours (Figure 5A). Pericytes, however, formed similar structures within 6–12 hours of seeding (Figure 5B). To illustrate the reciprocal influence between pericytes and endothelial cells (ECs), dye-labeled pericytes (PKH67, green) and HUVECs (PKH26, red) were mixed and co-cultured in 2D Matrigel, which resulted in the formation within 6–12 hours of capillary-like structures that included both cell types (Figure 5C). Pericytes (green) were observed to collocate with HUVECs (red) in the co-formed three-dimensional structures after incubation for 24 hours (Figure 5C, inset). Additionally, HUVECs (red) appeared to morphologically align with pericytes (green) (Figure 5D). To further unveil the vascular supportive role of pericytes, an *in vitro* 3D Matrigel system designed to simulate native capillary formation was used. HUVECs evenly distributed within the 3D Matrigel plug were unable to form organized structures after 72 hours (Figure 5E). To the contrary, pericytes started to form capillary-like networks 24 hours after gel-casting, with structural remodeling over time (Figure 5F). The dynamic interaction between pericytes and ECs was best depicted by encapsulating dye-labeled pericytes (green) and HUVECs (red) in a 3D Matrigel plug. Together these two types of cells formed capillary-like structures after incubation for 72 hours (Figure 5G) with pericytes surrounding HUVECs (Figure 5H). These data suggest that pericytes retained vascular cell features and formed structures supportive of microvascular networks even after purification and long-term culture, while pericyte-EC association may play a role in the pericyte-facilitated angiogenic process.

### Differential Expression of Pro-angiogenic Factors and Associated Receptors by Pericytes under Hypoxia

The paracrine angiogenic potential of pericytes in the ischemic heart was investigated using the simulated hypoxic environment *in vitro*. Expression of genes encoding pro-angiogenic factors and corresponding receptors was assessed by real-time qPCR. Vascular endothelial growth factor-A (VEGF-A), platelet-derived growth factor- $\beta$  (PDGF- $\beta$ ), and transforming growth factor (TGF)- $\beta$ 1 were notably up-regulated by 307% ( $p=0.001$ ), 437% ( $p=0.067$ ), and 178% ( $p=0.037$ ) respectively in pericytes cultured under hypoxic conditions (Figure 6A). Expression of other pro-angiogenic factors, including basic fibroblast growth factor (bFGF), hepatocyte growth factor (HGF), and epidermal growth factor (EGF), was down-regulated to 44% ( $p<0.05$ ), 23% ( $p=0.001$ ), and 60% ( $p>0.05$ ) of their expression levels in normoxia (Figure 6A). On the other hand, VEGF receptor-1 (VEGFR-1/Flt-1) and -2 (VEGFR-2/KDR/Flk-1) were substantially up-regulated by 458% ( $p=0.004$ ) and 572% ( $p=0.001$ ) respectively under 2.5% oxygen (Figure 6B). PDGF receptor- $\beta$  (PDGF-R $\beta$ ) expression was not significantly changed (161%,  $p>0.05$ ) (Figure 6B). VEGF secretion by pericytes, measured by ELISA, significantly increased over 3-fold ( $p=0.001$ ) under hypoxic culture conditions while angiopoietin-1 (Ang-1) secretion reduced by 35% ( $p>0.05$ ) (Figure 6C). Very little secretion of angiopoietin-2 (Ang-2) by pericytes was detected under both conditions ( $p>0.05$ ) (Figure 6C). Additionally, TGF- $\beta$ 1 secretion increased by 30.1% under hypoxia ( $p=0.028$ ) (Figure 6C), consistent with its up-regulated gene expression. The expression of human VEGF<sub>165</sub> by engrafted pericytes within the infarct region was confirmed by immunohistochemistry (Figure 6D, a–c).

## Transplanted Pericytes Home to Perivascular Locations

It is not known whether purified pericytes home back to perivascular areas *in vivo*. To reveal their engraftment and homing pattern, cultured pericytes were transduced with a GFP reporter gene at near 95% efficiency (Figure 7A) and injected ( $3.0 \times 10^5$  cells) into acutely infarcted hearts. GFP-labeled pericytes engrafted throughout the ventricular myocardium (Figure 7B), particularly in the peri-infarct area (Supplemental Figure S6). Many donor pericytes retained expression of NG2, a pericyte marker (Supplemental Figure S7). Confocal microscopy showed that a fraction of pericytes were identified in perivascular positions, adjacent to host CD31-positive endothelial cells (Figure 7C). Indeed, pericytes were aligned with (Figure 7C, main) or surrounding (Figure 7C, inset) CD31-positive microvessels, suggestive of perivascular homing. The number of engrafted GFP-positive pericytes was approximately  $9.1 \pm 1.3\%$  of total injected cells at the first week and declined over time to  $3.4 \pm 0.5\%$  at 8 weeks post-infarction ( $N=3$  per time point) (Figure 7D, dash-dot line). The perivascular homing rate instead increased from 28.6% to 40.1% over the course of 8 weeks, implicating the merit of niche-homing for long-term donor cell survival (Figure 7D, solid line). To demonstrate cellular interactions between donor pericytes and host ECs, we performed immunohistochemical studies for ephrin type-B receptor 2 (EphB2) and connexin43, a gap junction protein. Confocal images revealed that some GFP-positive pericytes juxtaposing host ECs expressed human-specific EphB2 (Figure 7E) or formed gap junctions with ECs (Figure 7F). These results suggest cellular interactions between host ECs and donor pericytes homed to perivascular locations.

## Cell Lineage Fate of Transplanted Pericytes

GFP-labeled pericytes were employed to track cell lineages developed from donor pericytes and investigate the capacity of human muscle pericytes to reconstitute major cardiac cell types after injury. Immunohistochemistry was performed to simultaneously detect GFP and cell lineage markers: the cardiomyocyte marker, cardiac troponin-I (cTn-I); the smooth muscle cell (SMC) marker, smooth muscle myosin heavy chain (SM-MHC); the endothelial cell (EC) marker, CD31. Confocal microscopy revealed that in the peri-infarct area, a minor fraction of transplanted pericytes co-express GFP and cTn-I (Supplemental Figure S8A–C, main), a few of which appear single-nucleated (Supplemental Figure S8A–C, inset). Some GFP-positive cardiomyocytes were identified within the remaining myocardium (Supplemental Figure S8D–F) with organized sarcomeric patterns (Supplemental Figure S8G–I). A very small number of donor pericytes co-expressed GFP and human-specific CD31 ( $<1\%$ ) (Supplemental Figure S8J–L). Similarly, co-expression of GFP and human-specific SM-MHC was detected in very few transplanted cells ( $<0.5\%$ ) (Supplemental Figure S8M–O). Negative control images were stained only with matching fluorescence-conjugated secondary antibodies (Supplemental Figure S8P–R).

## Discussion

Pericytes constitute a major structural component of small blood vessels, regulating vascular development, integrity and physiology. The recent identification of microvascular pericytes as one of the native sources of MSC ancestors raised the possibility that these cells participate in the repair of injured/ageing organs [11–16,35]. The therapeutic potential of microvascular pericytes was indicated by structural and functional regeneration of skeletal muscle involving direct pericyte differentiation into regenerative units as well as applications in lung repair and vascular tissue engineering [8,11,12,35,36]. Pericytes can also repair tissue via secretion of trophic factors, implying broad usage in clinical settings [8,18].

Recent studies indicated a possible developmental hierarchy among different stem/progenitor cell populations residing in the blood vessel walls [15,37]. Katare et al. reported that transplantation of adventitial progenitor cells repairs infarcted hearts through angiogenesis involving microRNA-132 [38]. Herein we demonstrate that transplantation of human FACS-purified microvascular pericytes contributes to the functional and structural repair of the ischemic heart, albeit unequally, through both paracrine effects and cellular interactions. A major goal of SCT, the prevention of progressive LV dilatation and consequent heart failure, was largely achieved by pericyte treatment, implicating the attenuation of deleterious remodeling. We also observed significant improvement of cardiac contractility in an acute infarction milieu, with up to 70% of healthy contractile function consistently maintained for at least two months. No significant difference was observed between adult and fetal pericytes in terms of heart repair. The therapeutic benefits observed could be explained, at least in part, by anti-fibrotic, anti-inflammatory, angiogenic, and to a lesser extent, cardiomyogenic properties of pericytes.

The anti-fibrotic action of mesodermal stem/progenitor cells in the injured heart has been reported [25–27]. MSC-conditioned medium diminished viability, proliferation, collagen synthesis, and  $\alpha$ -SMA expression in cardiac fibroblasts but stimulated MMP2/9 activities, indicating a paracrine anti-fibrotic property of MSCs [26,27]. Our results demonstrated a near 50% reduction of myocardial fibrosis following pericyte injection. Along with the attenuation of progressive LV dilatation, pericyte treatment appears to result in propitious remodeling, leading to improved myocardial compliance and strengthening of the ischemic cardiac tissue.

We speculated that decreased fibrosis/scar formation is, at least partially, associated with a reduced number of fibrotic cells resulting from the administration of pericytes. Interestingly, pericyte-treated hearts contained significantly less cells within the infarct area than PBS-injected controls ( $p < 0.05$ , Supplemental Figure S9A) with no statistical difference in Ki-67(+) proliferating cell density ( $p = 0.808$ , Supplemental Figure S9B). Additionally, TUNEL staining revealed no significant difference between pericyte- and PBS-injected hearts in the number of apoptotic cells within the infarct region ( $p = 0.296$ , Supplemental Figure S10A–B). Due to the highly fibrotic nature of MI, we were unable to quantitate fibrotic cells *in vivo*. Nevertheless, murine fibroblast proliferation was notably inhibited when cultured in hypoxic pericyte-conditioned medium *in vitro*, indicating the paracrine fibrosuppressive effect of pericytes under hypoxia. MMPs were suggested to play important roles in post-injury scar remodeling, angiogenesis, and vascular cell proliferation/migration [27,39]. In particular, a preponderant role of MMP-2 in preventing collagen accumulation by cardiac fibroblasts was proposed [27]. Consequently, we postulated the existence of a fibrolytic activity from donor pericytes, involving MMPs, which contributes to the attenuation of cardiac fibrosis. Indeed, high expression of MMP-2, but not MMP-9, by pericytes, even under hypoxic conditions, was observed. The expression of MMP-2 was confirmed in some, but not all, transplanted pericytes, implying a minor role of pericyte-mediated fibrolysis. Overall, our data suggest that the gross amelioration of fibrosis presumably involves decreased collagen deposition, reduced proliferation of fibroblasts, and altered remodeling of the extracellular matrix (ECM). Yet whether there exists one or more determining mechanism(s) remains to be investigated.

The immunosuppressive potential of MSCs, demonstrated by inhibiting T-lymphocyte proliferation in culture and counteracting graft-versus-host reaction in recipients of allogeneic blood stem cells, is currently exploited in clinical trials [28,29]. In the cardiac milieu, MSC transplantation in a rat model of acute myocarditis mitigated the increase in CD68+ phagocytic cells [40]. In the present study, pericyte treatment significantly diminished host monocyte/macrophage infiltration in the infarcted myocardium, suggesting

an anti-inflammatory potential which contributed to the reduction of fibrosis, amelioration of adverse remodeling, and improvement of cardiac function. Nevertheless, whether pericytes inhibit the acute-phase inflammation occurring soon after the incidence of MI is unknown. Inhibition of murine macrophage proliferation in culture by pericyte-conditioned medium suggests a paracrine mechanism of their immunomodulatory capacity.

The immunosuppressive and anti-inflammatory capacities of MSCs are primarily attributed to soluble factors/molecules, as IL-6, LIF, and HMOX-1 were shown to exercise beneficial immunosuppressive effects [28,29]. The attenuation of intense inflammation and mitigation of multi-organ damage by MSCs during sepsis are dependent on monocyte/macrophage-derived cytokines and regulated via PGE<sub>2</sub> signaling [41]. The immunoregulatory and cardioprotective functions of these molecules appear to be similar in the cardiac milieu [22,42]. Our data demonstrate that pericytes express high levels of IL-6, LIF, COX-2, HMOX-1, and HIF-1 $\alpha$ , which are sustained under hypoxic conditions. MCP-1 expression, however, notably decreased under hypoxia, corresponding with the reduced CD68<sup>+</sup> cell infiltration *in vivo*. Little to no expression of pro-inflammatory cytokines including IL-1 $\alpha$ , TNF- $\alpha$  and IFN $\gamma$  was detected. Virtually no expression of IL-4, IL-10, iNOS, and 2,3-IDO was observed in pericytes, suggestive of an immunoregulatory cytokine secretome that is unique to human microvascular pericytes [29,43]. Intriguingly, TGF- $\beta$ 1, also an anti-inflammatory yet fibrogenic cytokine, was strongly expressed by pericytes [22,44]. Our data suggested increased TGF- $\beta$ 1 expression/secretion by pericytes under hypoxic conditions (Figure 6A and 6C). Given the multiple functions each proposed growth factor/cytokine possesses, it is likely that a dynamic, interactive, and intricately orchestrated balance of trophic factors between donor and host cells holds the key to a successful ischemic tissue remodeling and regeneration.

A linear correlation between secretion of pro-angiogenic factors, angiogenesis and cardiac restoration was illustrated by blocking the bioactivity of VEGF secreted from transplanted murine muscle-derived stem cells in a mouse MI model, which not only abolished their stimulation of neovascularization but in turn negatively influenced LV contractility and infarct size [45]. Okada et al. further delineated the superior angiogenic properties of human myoendothelial progenitor cells and increased secretion of VEGF in response to hypoxia [34]. Given the indigenous vascular association of pericytes, we hypothesized that pericytes are able to repair the damaged host vasculature. Indeed, upon pericyte treatment, we observed a significantly larger host microvascular network not only in the peri-infarct collateral circulation but within the infarct region. Cultured pericytes secrete growth factors/cytokines/chemokines related to vascular physiology and remodeling [18]; among which, only VEGF-A, PDGF- $\beta$ , and TGF- $\beta$ 1 were substantially up-regulated under hypoxia, suggesting their role in pericyte-enhanced angiogenesis [39,46].

Angiogenesis may follow cell-cell contact between donor pericytes and host ECs, in addition to stimulation by angiogenic factors. Recent studies reported that MSCs and vascular mural/adventitial cells support ECs in small blood vessel formation and maturation in culture and *in vivo* [33,47]. We did observe the perivascular homing of donor pericytes in the ischemic heart. Some donor pericytes juxtaposing host ECs expressed interactive molecules including EphB2 and connexin43, suggestive of cellular interactions [48,49]. Planar Matrigel culture confirmed the vascular cell characteristics of pericytes and their capability to enhance the angiogenic behavior of ECs. We further demonstrated microvessel formation and vascular support by pericytes in three-dimensional cultures, indicating that associations between pericytes and ECs may contribute to revascularization. Nevertheless, the vibrant angiogenic response of pericytes observed *in vitro* may be reduced *in vivo* because of the harsh microenvironment caused by post-MI ischemia and inflammation.

Altogether, these results demonstrate that the angiogenic properties of pericytes may result from indirect paracrine effects and, albeit minor, direct cellular interactions.

Compared to other types of stem/progenitor cells, pericytes appear to engraft well in the infarcted heart initially, presumably attributable to several factors [50]. We did not observe apparent cell death of pericytes cultured under 2.5% O<sub>2</sub> for up to 48 hours, implying their resistance to hypoxia (data not shown). The increased proliferation and migration of pericytes in response to low oxygen concentration and ECM degradation products have important implications for ischemic injury repair [10]. The perivascular niche-homing capacity may further benefit the long-term survival of pericytes. Nonetheless, it remains unclear whether pericytes actively migrated to perivascular locations or served as a re-vascularizing center inducing/recruiting angiogenic proliferation/migration of host ECs. Future studies are needed to reveal the kinetics of pericyte-EC interaction and migration *in vivo*.

The potential of human muscle pericytes to reconstitute major cell types in the injured myocardium, though to a small extent, was hereby demonstrated. Cell fate tracking suggests that a minor fraction of donor pericytes differentiated into and/or fused with cardiomyocytes. Given the small number of GFP-cTnI dual-positive cells present, it is unlikely that these cells contributed significantly to functional recovery [21]. Pericytes, all of which were  $\alpha$ -SMA-positive during culture expansion, lost  $\alpha$ -SMA expression once homing to host microvasculature (data not shown), consistent with our finding that a subset of native microvascular pericytes do not express  $\alpha$ -SMA *in situ* [12].

In summary, FACS-purified human microvascular pericytes contribute to anatomic and functional cardiac improvement post-infarction through multiple cardioprotective mechanisms: reverse of ventricular remodeling, reduction of cardiac fibrosis, diminution of chronic inflammation, and promotion of host angiogenesis. Vessel-homing and small-scale regenerative events by pericytes partially reconstitute lost cardiac cells and contribute to the structural recovery. These cardioprotective and cardioregenerative activities of a novel stem cell population that can be purified to homogeneity and expanded *in vitro* await further research and exploitation in ischemic cardiovascular diseases.

## Supplementary Material

Refer to Web version on PubMed Central for supplementary material.

## Acknowledgments

The authors wish to thank Alison Logar for excellent technical assistance with flow cytometry, Dr. Bin Sun for expert assistance in real-time qPCR, Dr. Simon Watkins for confocal microscopy, Dr. Bing Wang for lentiviral-GFP vectors, James H. Cummins for editorial assistance, as well as Bolat Sultankulov and Damel Mektepbaeva for insightful discussion. This work was supported by grants from the Commonwealth of Pennsylvania (B.P.), National Institute of Health R01AR49684 (J.H.) and R21HL083057 (B.P.), the Henry J. Mankin Endowed Chair (J.H.), the William F. and Jean W. Donaldson Endowed Chair (J.H.), and the Ministry of Education and Science of the Republic of Kazakhstan (A.S.). C.W.C. was supported in part by the American Heart Association predoctoral fellowship. M. Corselli was supported by the California Institute for Regenerative Medicine training grant (TG2-01169).

## References

1. American Heart Association. Heart Disease and Stroke Statistics--2011 Update: A Report From the American Heart Association. *Circulation*. Feb 1; 2011 123(4):e18–209. [PubMed: 21160056]
2. Kumar, V.; Fausto, N.; Abbas, A. Robbins & Cotran Pathologic Basis of Disease. 7. Philadelphia, PA: Saunders; 2004.



3. Hansson EM, Lindsay ME, Chien KR. Regeneration Next: Toward Heart Stem Cell Therapeutics. *Cell Stem Cell*. 2009; 5(4):364–377. [PubMed: 19796617]
4. Segers VFM, Lee RT. Stem-cell therapy for cardiac disease. *Nature*. 2008; 451(7181):937–942. [PubMed: 18288183]
5. Janssens S. Stem Cells in the Treatment of Heart Disease. *Annual Review of Medicine*. 2010; 61(1):287–300.
6. Menasche P. Cardiac cell therapy: Lessons from clinical trials. *Journal of Molecular and Cellular Cardiology*. 2011; 50(2):258–265. [PubMed: 20600097]
7. Armulik A, Abramsson A, Betsholtz C. Endothelial/pericyte interactions. *Circ Res*. 2005; 97(6):512–523. [PubMed: 16166562]
8. Montemurro T, Andriolo G, Montelatici E, et al. Differentiation and migration properties of human foetal umbilical cord perivascular cells: potential for lung repair. *Journal of Cellular and Molecular Medicine*. 2011; 15(4):796–808. [PubMed: 20219017]
9. Park TS, Gavina M, Chen C-W, et al. Placental Perivascular Cells for Human Muscle Regeneration. *Stem Cells and Development*. 2011; 20(3):451–463. [PubMed: 20923371]
10. Tottey S, Corselli M, Jeffries EM, Londono R, Peault B, Badylak SF. Extracellular Matrix Degradation Products and Low-Oxygen Conditions Enhance the Regenerative Potential of Perivascular Stem Cells. *Tissue Engineering Part A*. 2011; 17(1–2):37–44. [PubMed: 20653348]
11. Dellavalle A, Sampaolesi M, Tonlorenzi R, et al. Pericytes of human skeletal muscle are myogenic precursors distinct from satellite cells. *Nat Cell Biol*. 2007; 9(3):255–267. [PubMed: 17293855]
12. Crisan M, Yap S, Casteilla L, et al. A Perivascular Origin for Mesenchymal Stem Cells in Multiple Human Organs. *Cell Stem Cell*. 2008; 3(3):301–313. [PubMed: 18786417]
13. Sacchetti B, Funari A, Michienzi S, et al. Self-Renewing Osteoprogenitors in Bone Marrow Sinusoids Can Organize a Hematopoietic Microenvironment. *Cell*. 2007; 131(2):324–336. [PubMed: 17956733]
14. Feng J, Mantesso A, De Bari C, Nishiyama A, Sharpe PT. Dual origin of mesenchymal stem cells contributing to organ growth and repair. *Proceedings of the National Academy of Sciences*. Apr 19; 2011 108(16):6503–6508.
15. Corselli M, Chen C-W, Sun B, Yap S, Rubin PJ, Peault B. The tunica adventitia of human arteries and veins as a source of mesenchymal stem cells. *Stem Cells and Development*. 2011; 21(8):1299–1308. [PubMed: 21861688]
16. Tormin A, Li O, Brune JC, et al. CD146 expression on primary nonhematopoietic bone marrow stem cells is correlated with in situ localization. *Blood*. May 12; 2011 117(19):5067–5077. [PubMed: 21415267]
17. Corselli M, Chen CW, Crisan M, Lazzari L, Peault B. Perivascular ancestors of adult multipotent stem cells. *Arterioscler Thromb Vasc Biol*. Jun; 2010 30(6):1104–1109. [PubMed: 20453168]
18. Chen CW, Montelatici E, Crisan M, Corselli M, Huard J, Lazzari L, Péault B. Perivascular multi-lineage progenitor cells in human organs: regenerative units, cytokine sources or both? *Cytokine Growth Factor Rev*. 2009; 20(5–6):429–434. [PubMed: 19926515]
19. James A, Zara J, Zhang X, et al. Perivascular Stem Cells: A Prospectively Purified Mesenchymal Stem Cell Population for Bone Tissue Engineering. *Stem Cells*. 2012 In press.
20. Chen CW, Okada M, Tobita K, Peault B, Huard J. Purified Human Muscle-derived Pericytes Support Formation of Vascular Structures and Promote Angiogenesis After Myocardial Infarction. *Circulation*. 2009; 120:S1053.
21. Gnechchi M, Zhang Z, Ni A, Dzau VJ. Paracrine Mechanisms in Adult Stem Cell Signaling and Therapy. *Circ Res*. Nov 21; 2008 103(11):1204–1219. [PubMed: 19028920]
22. Frangogiannis NG. The immune system and cardiac repair. *Pharmacological Research*. 2008; 58(2):88–111. [PubMed: 18620057]
23. Caplan AI, Dennis JE. Mesenchymal stem cells as trophic mediators. *Journal of Cellular Biochemistry*. 2006; 98(5):1076–1084. [PubMed: 16619257]
24. Berry MF, Engler AJ, Woo YJ, et al. Mesenchymal stem cell injection after myocardial infarction improves myocardial compliance. *Am J Physiol Heart Circ Physiol*. Jun 1; 2006 290(6):H2196–2203. [PubMed: 16473959]

25. Pittenger MF, Martin BJ. Mesenchymal Stem Cells and Their Potential as Cardiac Therapeutics. *Circ Res.* Jul 9; 2004 95(1):9–20. [PubMed: 15242981]
26. Ohnishi S, Sumiyoshi H, Kitamura S, Nagaya N. Mesenchymal stem cells attenuate cardiac fibroblast proliferation and collagen synthesis through paracrine actions. *FEBS Letters.* 2007; 581(21):3961–3966. [PubMed: 17662720]
27. Mias C, Lairez O, Trouche E, et al. Mesenchymal stem cells promote matrix metalloproteinase secretion by cardiac fibroblasts and reduce cardiac ventricular fibrosis after myocardial infarction. *Stem Cells.* Nov; 2009 27(11):2734–2743. [PubMed: 19591227]
28. Ghannam S, Bouffi C, Djouad F, Jorgensen C, Noel D. Immunosuppression by mesenchymal stem cells: mechanisms and clinical applications. *Stem Cell Res Ther.* 2010; 1(1):2. [PubMed: 20504283]
29. Shi Y, Hu G, Su J, et al. Mesenchymal stem cells: a new strategy for immunosuppression and tissue repair. *Cell Res.* May; 2010 20(5):510–518. [PubMed: 20368733]
30. Renault MA, Losordo DW. Therapeutic myocardial angiogenesis. *Microvasc Res.* 2007; 74(2–3):159–171. [PubMed: 17950369]
31. Sieveking DP, Ng MKC. Cell therapies for therapeutic angiogenesis: back to the bench. *Vasc Med.* 2009; 14(2):153–166. [PubMed: 19366823]
32. Saunders WB, Bohnsack BL, Faske JB, et al. Coregulation of vascular tube stabilization by endothelial cell TIMP-2 and pericyte TIMP-3. *The Journal of Cell Biology.* Oct 9; 2006 175(1):179–191. [PubMed: 17030988]
33. Au P, Tam J, Fukumura D, Jain RK. Bone marrow-derived mesenchymal stem cells facilitate engineering of long-lasting functional vasculature. *Blood.* 2008; 111(9):4551–4558. [PubMed: 18256324]
34. Okada M, Payne TR, Zheng B, et al. Myogenic Endothelial Cells Purified From Human Skeletal Muscle Improve Cardiac Function After Transplantation Into Infarcted Myocardium. *Journal of the American College of Cardiology.* 2008; 52(23):1869–1880. [PubMed: 19038685]
35. Dellavalle A, Maroli G, Covarello D, et al. Pericytes resident in postnatal skeletal muscle differentiate into muscle fibres and generate satellite cells. *Nat Commun.* 2011; 2:499. [PubMed: 21988915]
36. He W, Nieponice A, Soletti L, et al. Pericyte-based human tissue engineered vascular grafts. *Biomaterials.* 2010; 31(32):8235–8244. [PubMed: 20684982]
37. Zimmerlin L, Donnenberg VS, Pfeifer ME, et al. Stromal vascular progenitors in adult human adipose tissue. *Cytometry A.* Jan; 2010 77(1):22–30. [PubMed: 19852056]
38. Katare R, Riu F, Mitchell K, et al. Transplantation of Human Pericyte Progenitor Cells Improves the Repair of Infarcted Heart Through Activation of an Angiogenic Program Involving Micro-RNA-132/Novelty and Significance. *Circulation Research.* Sep 30; 2011 109(8):894–906. [PubMed: 21868695]
39. Enciso JM, Hirschi KK. Understanding Abnormalities in Vascular Specification and Remodeling. *Pediatrics.* Jul 1; 2005 116(1):228–230. [PubMed: 15995057]
40. Ohnishi S, Yanagawa B, Tanaka K, et al. Transplantation of mesenchymal stem cells attenuates myocardial injury and dysfunction in a rat model of acute myocarditis. *Journal of Molecular and Cellular Cardiology.* 2007; 42(1):88–97. [PubMed: 17101147]
41. Nemeth K, Leelahavanichkul A, Yuen PS, et al. Bone marrow stromal cells attenuate sepsis via prostaglandin E(2)-dependent reprogramming of host macrophages to increase their interleukin-10 production. *Nat Med.* Jan; 2009 15(1):42–49. [PubMed: 19098906]
42. Liu X, Pachori AS, Ward CA, et al. Heme oxygenase-1 (HO-1) inhibits postmyocardial infarct remodeling and restores ventricular function. *Faseb J.* Feb; 2006 20(2):207–216. [PubMed: 16449792]
43. Ren G, Su J, Zhang L, et al. Species variation in the mechanisms of mesenchymal stem cell-mediated immunosuppression. *Stem Cells.* Aug; 2009 27(8):1954–1962. [PubMed: 19544427]
44. Abarbanell AM, Coffey AC, Fehrenbacher JW, et al. Proinflammatory cytokine effects on mesenchymal stem cell therapy for the ischemic heart. *Ann Thorac Surg.* Sep; 2009 88(3):1036–1043. [PubMed: 19699961]

45. Payne TR, Oshima H, Okada M, Momoi N, Tobita K, Keller BB, Peng H, Huard J. A relationship between vascular endothelial growth factor, angiogenesis, and cardiac repair after muscle stem cell transplantation into ischemic hearts. *J Am Coll Cardiol.* 2007; 50(17):1677–1684. [PubMed: 17950150]
46. Ohnishi S, Yasuda T, Kitamura S, Nagaya N. Effect of Hypoxia on Gene Expression of Bone Marrow-Derived Mesenchymal Stem Cells and Mononuclear Cells. *Stem Cells.* 2007; 25(5):1166–1177. [PubMed: 17289933]
47. Campagnolo P, Cesselli D, Al Haj Zen A, et al. Human Adult Vena Saphena Contains Perivascular Progenitor Cells Endowed With Clonogenic and Proangiogenic Potential. *Circulation.* Apr 20; 2010 121(15):1735–1745. [PubMed: 20368523]
48. Salvucci O, de la Luz Sierra M, Martina JA, McCormick PJ, Tosato G. EphB2 and EphB4 receptors forward signaling promotes SDF-1–induced endothelial cell chemotaxis and branching remodeling. *Blood.* Nov 1; 2006 108(9):2914–2922. [PubMed: 16840724]
49. Hirschi KK, Burt JM, Hirschi KD, Dai C. Gap Junction Communication Mediates Transforming Growth Factor- $\beta$  Activation and Endothelial-Induced Mural Cell Differentiation. *Circulation Research.* Sep 5; 2003 93(5):429–437. [PubMed: 12919949]
50. Wu KH, Mo XM, Han ZC, Zhou B. Stem Cell Engraftment and Survival in the Ischemic Heart. *The Annals of Thoracic Surgery.* 2011; 92(5):1917–1925. [PubMed: 21955573]

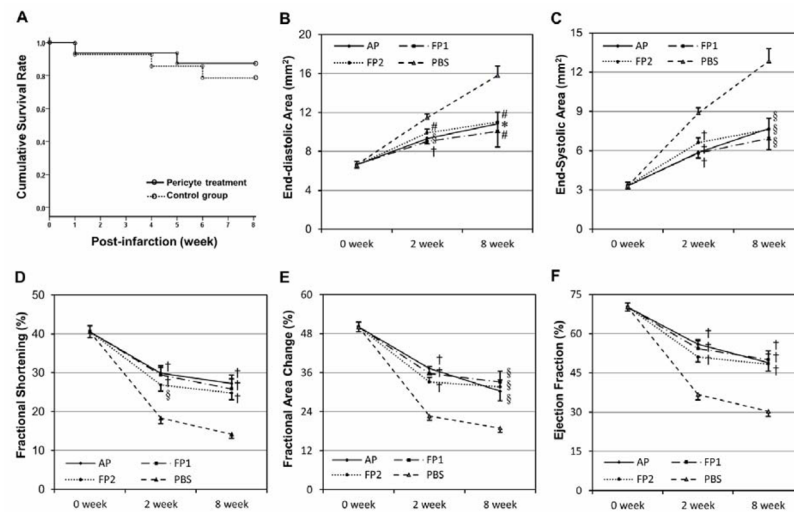


**Figure 1. Survival rate and cardiac functional assessment**

(A) Cumulative survival rate of the animals over 8 weeks post-surgery (Kaplan-Meier Survival Curve, log-rank test  $p=0.529$ ). Echocardiographic analyses revealed a significant reduction of LV dilatation by transplantation of all three pericyte populations (AP, FP1, and FP2), as shown by the smaller LV area in end-diastole (B) and end-systole (C) of hearts at both time points. Injection of pericytes also resulted in substantial improvement in LV contractility, as indicated by greater fractional shortening (D), fractional area change (E), and ejection fraction (F), at both time points.

(<sup>†</sup> $p$  0.001; <sup>§</sup> $p$  0.005; <sup>#</sup> $p$  0.01; <sup>\*</sup> $p$  0.05; versus PBS control group at each time point)

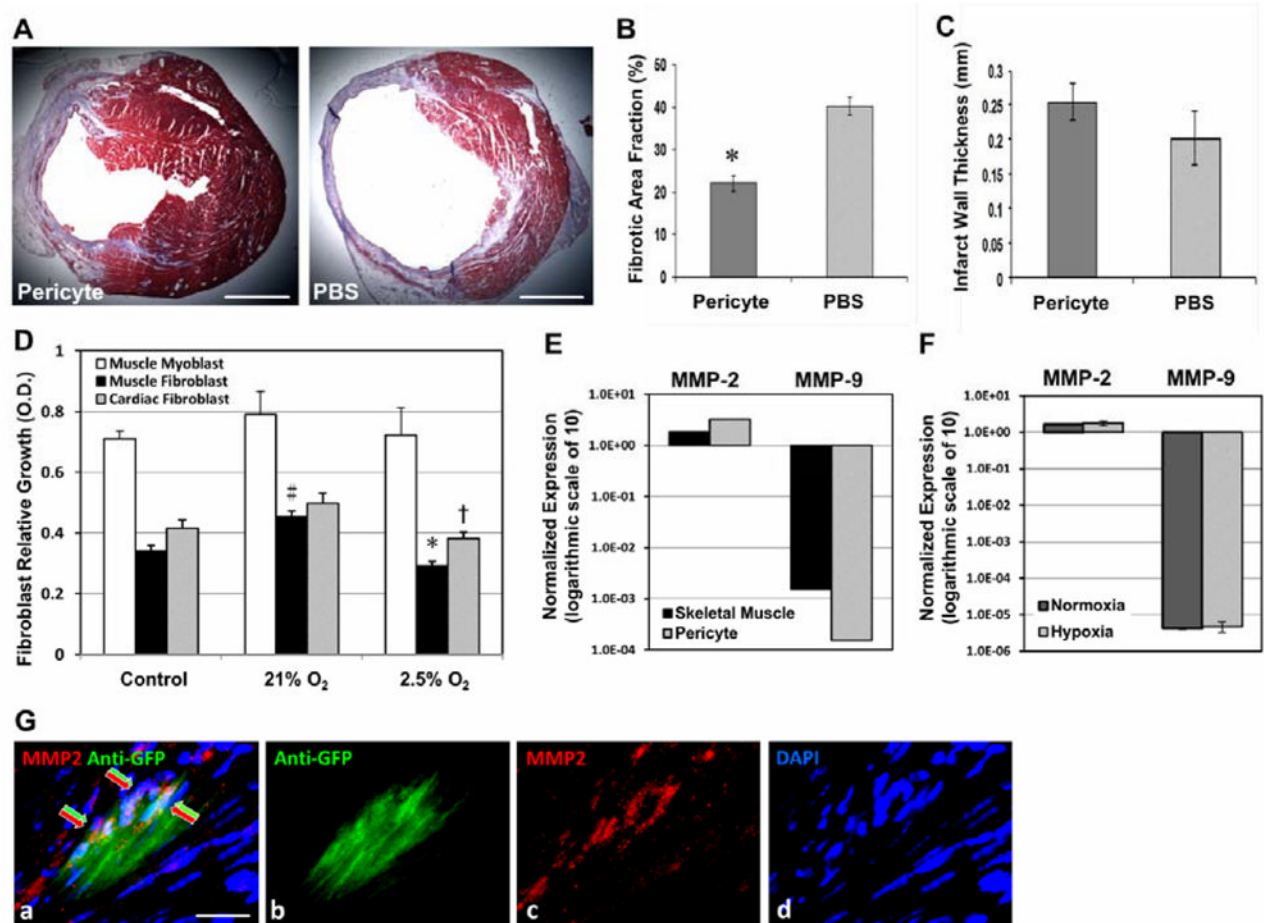


### Figure 2. Attenuation of myocardial fibrosis by pericyte treatment

(A) Masson's trichrome-stained transverse sections of hearts injected with pericytes or PBS (collagen in blue/purple, cardiac muscle in red; scale bars=1 mm). (B) The fibrotic area fraction was dramatically decreased in pericyte-injected hearts ( $p < 0.001$ ). (C) Pericyte group had no significant increase in the infarct wall thickness. (D) When culturing with hypoxic pericyte-conditioned medium (P-CM), the proliferation of murine cardiac fibroblasts was significantly reduced ( $^{\dagger}p=0.019$ , versus normoxic P-CM) while muscle fibroblast proliferation exhibited the same pattern ( $^{*}p<0.001$ ). Normoxic P-CM had a pro-proliferative effect over control medium in muscle fibroblasts, but not in cardiac fibroblasts ( $^{\#}p<0.05$ ). Skeletal myoblast proliferation was not significantly affected by either of the P-CMs. (E) Expression of MMP-2 in cultured pericytes was higher than that in skeletal muscle lysates. Conversely, MMP-9 expression in pericytes was nearly 10 times less (logarithmic scale of 10 in arbitrary fluorescence units). (F) Expression of both MMP-2 and -9 in pericytes did not change significantly under hypoxia ( $p>0.05$ , logarithmic scale of 10 in arbitrary fluorescence units). (G) Immunohistochemistry revealed MMP-2 expression (red arrows) by some of the GFP-labeled donor pericytes (green arrows) within the infarct area at 2 weeks post-infarction (a) merge (b) anti-GFP in green (c) MMP-2 in red (d) DAPI nuclei staining in blue (scale bar=20 $\mu$ m).



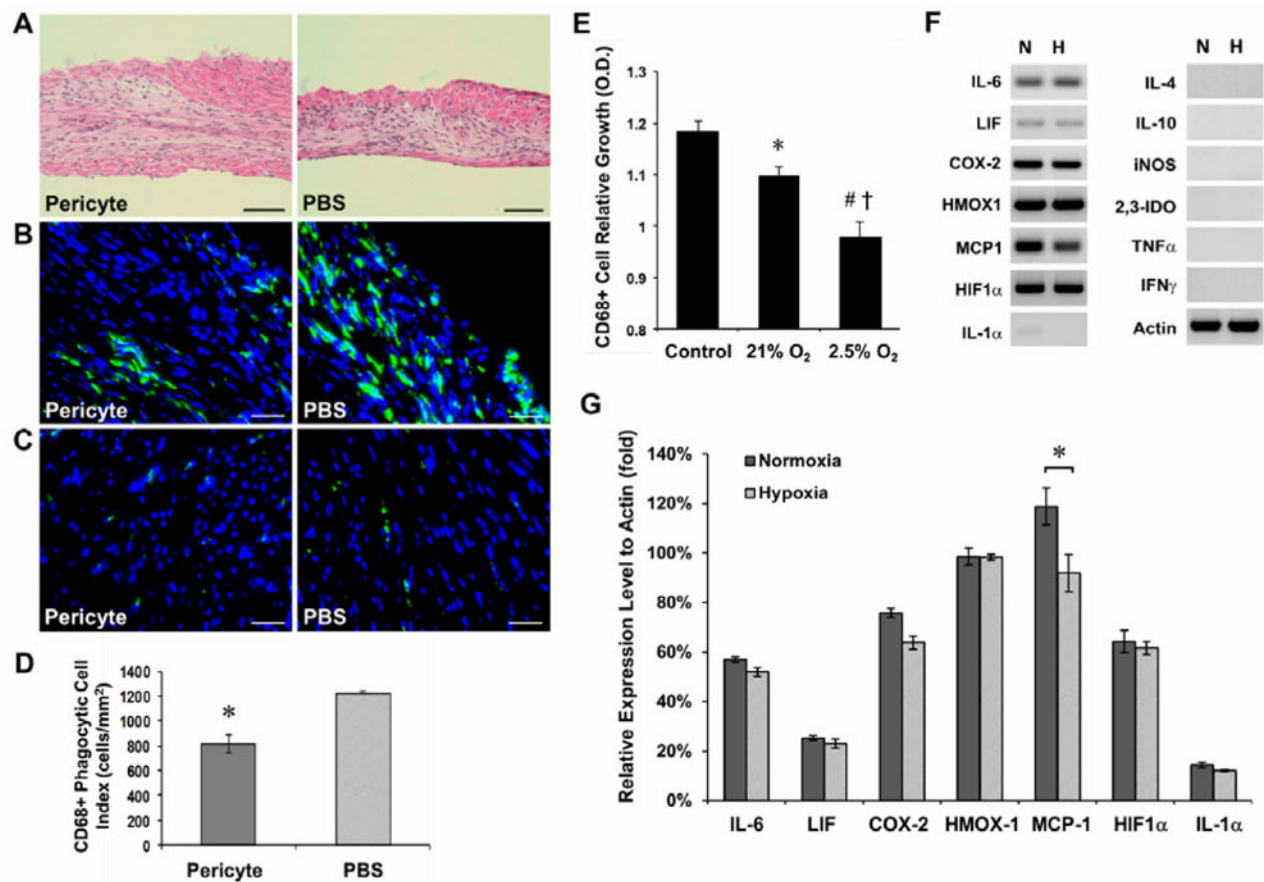


**Figure 3. Reduction of host phagocytic cell infiltration by pericyte transplantation**

(A) H&E staining revealed a greater focal infiltration of leukocytes (dark blue-stained nuclei) within the infarct region in PBS-injected controls at 2 weeks post-infarction (scale bars=100 $\mu$ m). (B) Anti-mouse CD68 immunostaining showed that the infarct region of pericyte-injected hearts contains less host phagocytic cells (scale bars=50 $\mu$ m). (C) Host CD68-positive cells were locally attracted to the infarct region but not to the unaffected myocardium (posterior ventricular wall) in both groups (scale bars=50 $\mu$ m). (D) Host monocytes/macrophage infiltration at the infarct site was significantly reduced ( $p<0.001$ ). (E) The proliferation of murine macrophages was significantly inhibited when culturing with pericyte-conditioned media ( $*p=0.018$ ,  $^{\#}p<0.001$ , versus control medium), an effect more prominent with hypoxic pericyte-conditioned medium ( $^{\dagger}p=0.002$ , hypoxia versus normoxia). (F) Cultured pericytes exhibited sustained, high expression of genes regulating the inflammatory responses, even under 2.5% O<sub>2</sub> (N: normoxia; H: hypoxia). Little expression of IL-1 $\alpha$  and no expression of IL-4, IL-10, iNOS, 2,3-IDO, TNF- $\alpha$ , and IFN $\gamma$  were detected. (G) No statistically significant difference in expression of genes of immunoregulatory molecules between normoxic- and hypoxic-cultured pericytes except MCP-1, which notably decreased in hypoxic cultures (sqRT-PCR analysis,  $p=0.027$ ).

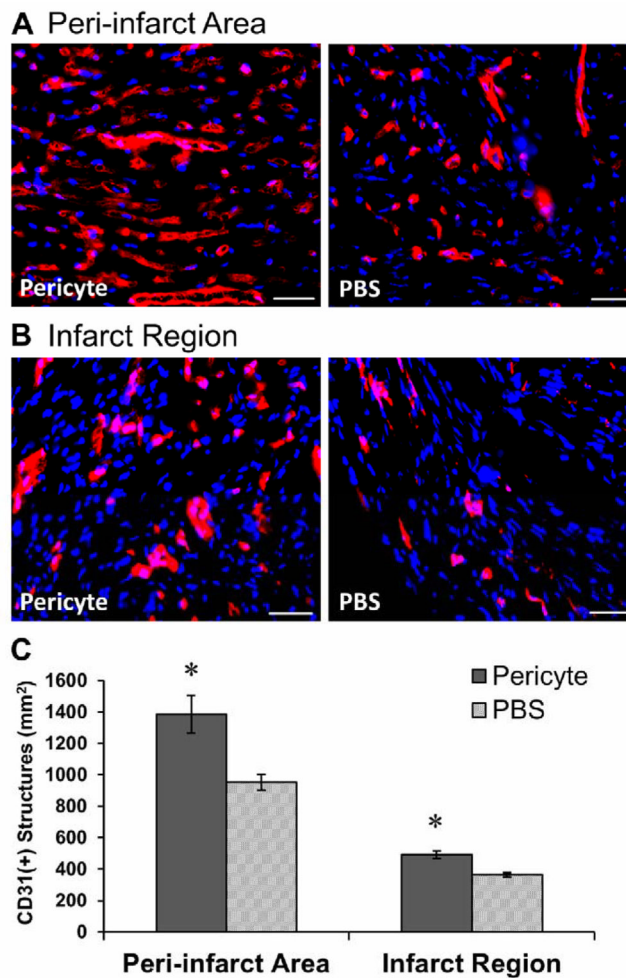


**Figure 4. Promotion of host angiogenesis by pericyte treatment**

Representative images of anti-mouse CD31 immunostaining (A) in the peri-infarct area and (B) within the infarct region of hearts injected with pericytes or PBS (scale bars=50μm). (C) Pericyte-treated hearts displayed significantly higher capillary densities in the peri-infarct area ( $p<0.05$ ) and within the infarct region ( $p<0.001$ ).

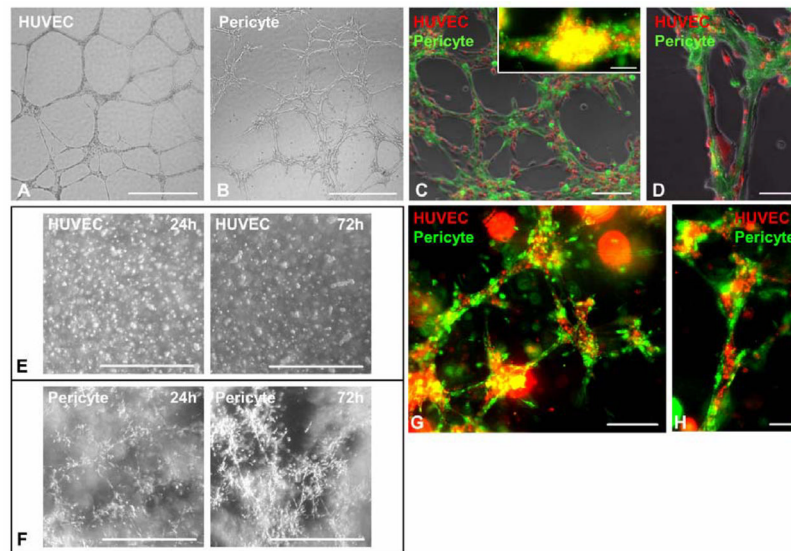


**Figure 5. Pericytes support microvascular structures**

(A) While HUVECs seeded onto Matrigel-coated wells formed typical capillary-like networks after 24 hours, (B) pericytes formed similar structures within 6–12 hours (scale bars=1mm). (C) When co-cultured on Matrigel, dye-labeled pericytes (green) and HUVECs (red) co-formed capillary-like networks within 6–12 hours, ([C], inset) with collocations of pericytes and HUVECs in three-dimensional structures formed 24 hours after seeding (scale bars: main=200 $\mu$ m; inset=100 $\mu$ m). (D) HUVECs (red) appear to line and spread out on top of the pericyte-formed structures (green) (scale bar=100 $\mu$ m). (E) To simulate native capillary formation, HUVECs were evenly encapsulated into 3D Matrigel plug for 72 hours but unable to form any organized structure (scale bars=1mm). (F) Pericytes instead formed capillary-like networks in Matrigel plug with structural organization and maturation over time (scale bars=1mm). (G) When dye-labeled pericytes (green) and HUVECs (red) were co-casted into the 3D-gel plug, the two types of cells formed microvessel-like networks within 72 hours, (H) with pericytes surrounding HUVECs (scale bars: G=200 $\mu$ m; H=50 $\mu$ m).

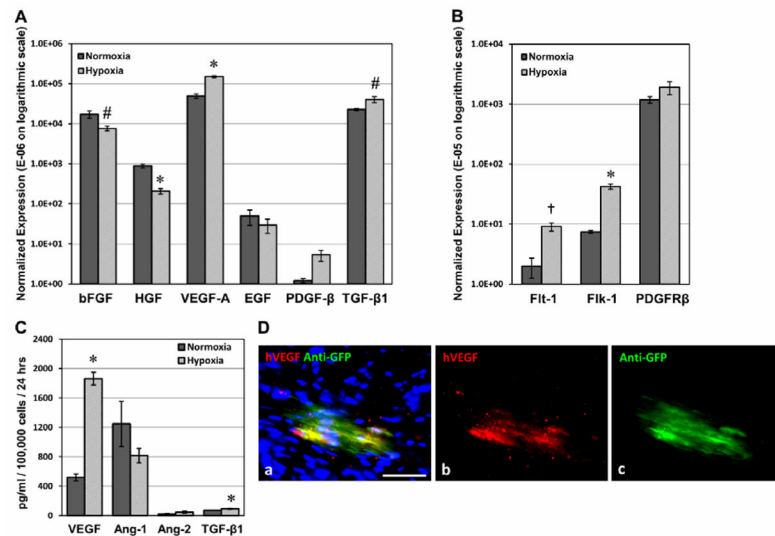


**Figure 6. Expression of pro-angiogenic factors and associated receptors under hypoxia**  
 (A) Pericytes dramatically up-regulated VEGF-A, PDGF-β, TGF-β1 gene expression under hypoxic conditions (2.5% O<sub>2</sub>) while expression of other pro-angiogenic factors, including bFGF, HGF and EGF were distinctively repressed. (B) Simultaneously, VEGFR-1 (Flt-1) and -2 (Flk-1) were substantially up-regulated, and PDGF-Rβ expression was moderately increased. All expression levels are normalized to human cyclophilin and presented in arbitrary fluorescence units on an expanded logarithmic scale (#*p*<0.05, \**p* 0.001, †*p*<0.01, hypoxia versus normoxia). (C) Significantly increased secretion of VEGF (*p* 0.001) and TGF-β1 (*p*=0.028) by pericytes under hypoxic culture conditions was detected by ELISA while secretion of Ang-1 was reduced by 35% (*p*>0.05). Very little secretion of Ang-2 was detected under both conditions (*p*>0.05). (D) Immunohistochemistry revealed human VEGF<sub>165</sub> expression by GFP-labeled donor pericytes within the infarct area at 2 weeks post-infarction (a) merge (b) hVEGF<sub>165</sub> in red (c) anti-GFP in green (scale bar=50μm).

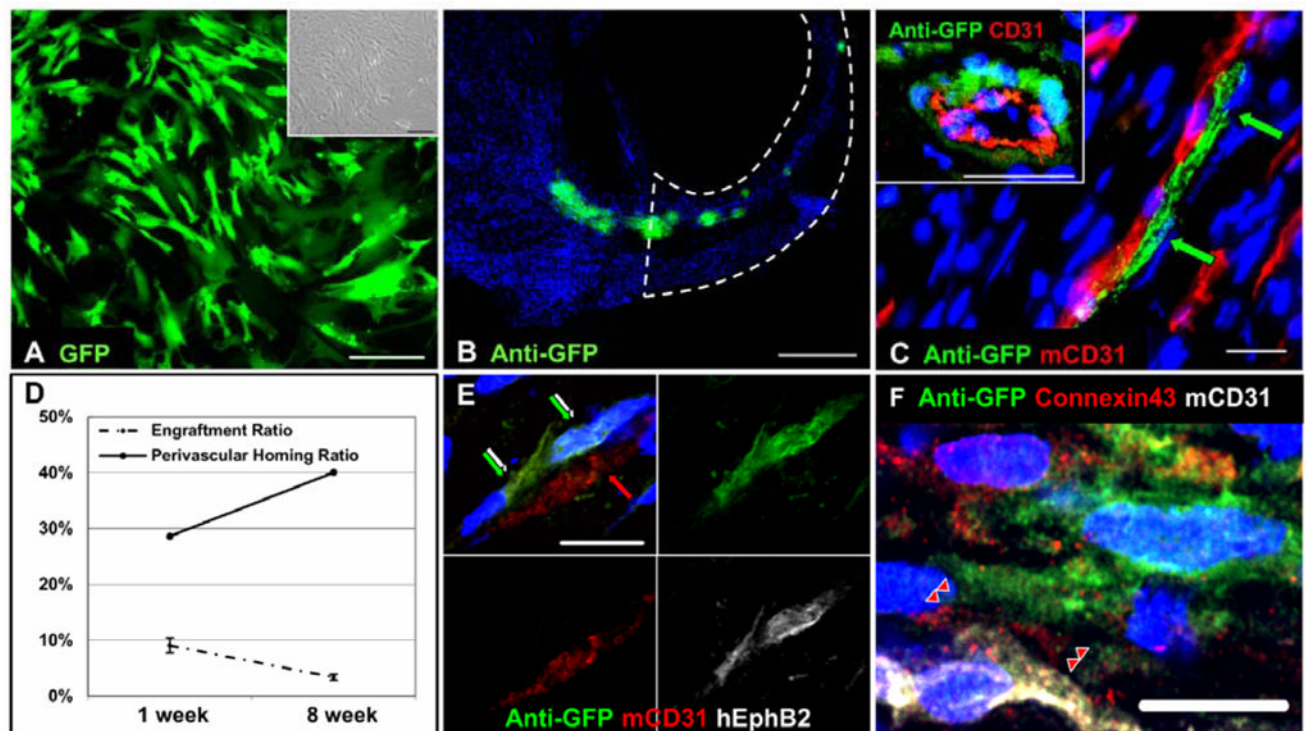


**Figure 7. Transplanted pericytes home to perivascular locations**

(A) Pericytes were transduced with GFP reporter at nearly 95% efficiency. Fluorescence ([A], main) and bright-field ([A], inset) images were taken from the same low-power field (scale bars=200 $\mu$ m). (B) Engraftment of GFP-labeled pericytes within host myocardium was revealed by anti-GFP immunostaining at 1 week post-injection (scale bar=500 $\mu$ m, infarct site encircled by dotted lines). (C) Pericytes were lining with ([C], main) or surrounding ([C], inset) host CD31-positive microvasculature (scale bars=20 $\mu$ m). (D) The engraftment efficiency of pericytes at 1 week ( $9.1 \pm 1.3\%$ ) and 8 weeks ( $3.4 \pm 0.5\%$ ) post-infarction was depicted (dash-dot line). The perivascular homing ratio instead increased from 28.6% to 40.1% and was delineated separately (solid line). Some GFP-positive pericytes juxtaposing host ECs (E) expressed human-specific EphB2 (green/white arrows) or (F) formed connexin43-positive gap junctions with ECs (red arrow heads) (scale bars=10 $\mu$ m).